Magnetic Resonance Insights

ORIGINAL RESEARCH

Magnetic Resonance Imaging-derived Flow Parameters for the Analysis of Cardiovascular Diseases and Drug Development

Dada O. Michael[1], Awojoyogbe O. Bamidele[1], Adesola O. Adewale[1] and Boubaker Karem[2]

[1]Department of Physics, Federal University of Technology, P.M.B. 65, Minna, Niger State, Nigeria.
[2]UPDS/ESSTT/63 Rue Sidi Jabeur, 5100 Mahdia, Tunisia.
Corresponding author email: awojoyogbe@yahoo.com

Abstract: Nuclear magnetic resonance (NMR) allows for fast, accurate and noninvasive measurement of fluid flow in restricted and non-restricted media. The results of such measurements may be possible for a very small B_0 field and can be enhanced through detailed examination of generating functions that may arise from polynomial solutions of NMR flow equations in terms of Legendre polynomials and Boubaker polynomials. The generating functions of these polynomials can present an array of interesting possibilities that may be useful for understanding the basic physics of extracting relevant NMR flow information from which various hemodynamic problems can be carefully studied. Specifically, these results may be used to develop effective drugs for cardiovascular-related diseases.

Keywords: Bloch NMR flow equations, NMR transverse magnetization, Legendre polynomials, Boubaker polynomials, rotational diffusion coefficient, cardiovascular diseases, drug discovery

Magnetic Resonance Insights 2013:6 83–93

doi: 10.4137/MRI.S12195

This article is available from http://www.la-press.com.

Introduction

Magnetic resonance imaging (MRI) is an imaging modality based on the principles of NMR and can be used to directly observe the movement of molecules associated with fluid flow. This provides for an excellent opportunity to noninvasively determine molecular velocities within a confined range, for example due to the formation of plaque in blood vessels.[1–3]

Traditionally, MRI generates exquisite images of the soft tissue anatomy of the human body. The principle of MRI is to record the variations of the nuclear magnetization of biological tissues using different kinds of magnetic fields.[1,2,4] A static magnetic field B_0 is used to generate a macroscopic nuclear magnetization $\overrightarrow{M}$ in the body. By applying an additional pulsed magnetic field $\overrightarrow{B}_1$ in the transverse plane, the orientation of $\overrightarrow{M}$ can be shifted into this plane as the precession is always around the total magnetic field $B = B_0 + B_1$. To investigate the variations of magnetization $\overrightarrow{M}$ in the presence of the field $\overrightarrow{B}_1$, it is convenient to use a rotating rather than static frame of reference. The frame is chosen to rotate at the same frequency as $\overrightarrow{B}_1$, such that both $\overrightarrow{B}_0$ and $\overrightarrow{B}_1$ become time-independent. The NMR Bloch flow equations in this frame can be expressed[5–8] by the equation:

$$V^2\frac{d^2M_y}{dx^2}+V\left(\frac{1}{T_1}+\frac{1}{T_2}\right)\frac{dM_y}{dx}+\left(\gamma^2B_1^2(x)+\frac{1}{T_1T_2}\right)M_y=\frac{M_0\gamma B_1(x)}{T_1} \quad (1)$$

with the following parameters: γ-gyromagnetic ratio of fluid spins, $\overrightarrow{M}_0$-equilibrium magnetization, T_1-spin lattice (longitudinal) relaxation time, T_2-spin-spin (transverse) relaxation time, V-variable flow velocity.

In order to calculate the transverse magnetization component $\overrightarrow{M}_y$, two reasonable initial boundary conditions which may conform to the real time experimental arrangements were chosen. These included the following.

i. $M_0 \neq M_x$, a condition which holds true in general and in particular when there is a small RF limit: $\gamma^2 B_1{}^2 T_1 T_2 << 1$. This is typically regarded as a linearity condition in which the frequency response takes on the characteristic Lorentzian form.[4]

ii. For this investigation, we assumed that the resonance condition existed at Larmor frequency:[7]

$$f_0 = \gamma B - \omega = 0 \quad (2a)$$

iii. Before entering the signal detector coil, fluid particles have magnetization of

$$M_x = 0 \quad \text{and} \quad M_y = 0 \quad (2b)$$

Under these conditions and for steady flow, we can write

$$\frac{\partial M_y}{\partial t} = 0 \quad (3)$$

When the RF $B_1(x)$ field is applied, M_y has the largest possible amplitude when RF $B_1(x)$ is maximum and $M_0 \approx 0$. At this point, when the maximum possible NMR signal amplitude is detected (maximum values of M_y and $B_1(x)$ respectively), equation (1) becomes:

$$\frac{d^2M_y}{dx^2}+\frac{T_0}{V(x)}\frac{dM_y}{dx}+\frac{1}{V^2(x)}\left(\gamma^2B_1^2(x)+\frac{1}{T_1T_2}\right)M_y=0 \quad (4)$$

where

$$T_0 = \frac{1}{T_1}+\frac{1}{T_2}. \quad (5)$$

In this study, we conducted a detailed analysis of generating functions that may arise from polynomial solutions of equation (4) in terms of Legendre polynomials and Boubaker polynomials.[9–12] The generating functions of these polynomials can enhance the present understanding of the basic physics required to extract relevant NMR flow information from which various hemodynamic problems can be studied.

Quantitative fluid flow imaging based on the solution of Bloch NMR flow equations in terms of Legendre polynomials and Boubaker polynomials is very important because significant applications of MRI techniques are based on the Bloch NMR equations. Applying appropriate mathematical techniques to solve Bloch NMR flow equations and extract

relevant NMR flow parameters to accurately monitor the fluid state is very important for MRI studies.

Mathematical Model

Equation (4) was obtained under conditions of when the RF $B_1(x)$ field is applied and M_y has a maximum value, $M_0 = 0$. Equation (4) can be written in the form:

$$\frac{d^2M_y}{dx^2} + \frac{T_0}{V(x)}\frac{dM_y}{dx} + \frac{T_g}{V^2(x)}M_y = 0 \qquad (6)$$

The fluid velocity V is dependent on the spatial variable x. We may therefore write that:

$$\frac{T_0}{V(x)} = \frac{1}{l}Cot\frac{x}{l} \qquad (7)$$

where $l = l(x)$ is a parameter in the unit of length and $Cot\frac{x}{l}$ is a cotangent function of $\frac{x}{l}$. Equation (6) is based on the condition that:

$$\gamma^2 B_1^2(x) << \frac{1}{T_1T_2} \qquad (8)$$

where

$$T_g = \frac{1}{T_1T_2}. \qquad (9)$$

Specifically, in this model, we consider a fluid particle confined to a limited range as shown in Figure 1.

At the point x_3, the fluid velocity $V(x)$ becomes virtually zero and the blockage stops the blood supply to the area, leading to ischemia (lack of oxygen) and eventually necrosis.

The fluid velocity is completely quantified within the (anatomical) range except at the points (certain discrete values μ, an NMR number associated with the NMR transverse magnetization and velocities) where μ is odd number because the velocity is infinite at these points (this typically occurs at bifurcations, ie, points x_1 and x_2).

Since the expression of equation (7) implies that the fluid velocity is a function of relaxation times, we can assume that V^2 is directly proportional to T_g such that:

$$\frac{V^2(x)}{T_g(x)} = \frac{1}{n(n+1)}l^2 \qquad (10)$$

where $\frac{1}{n(n+1)}$ is the constant of proportion (n is a positive integer parameter).

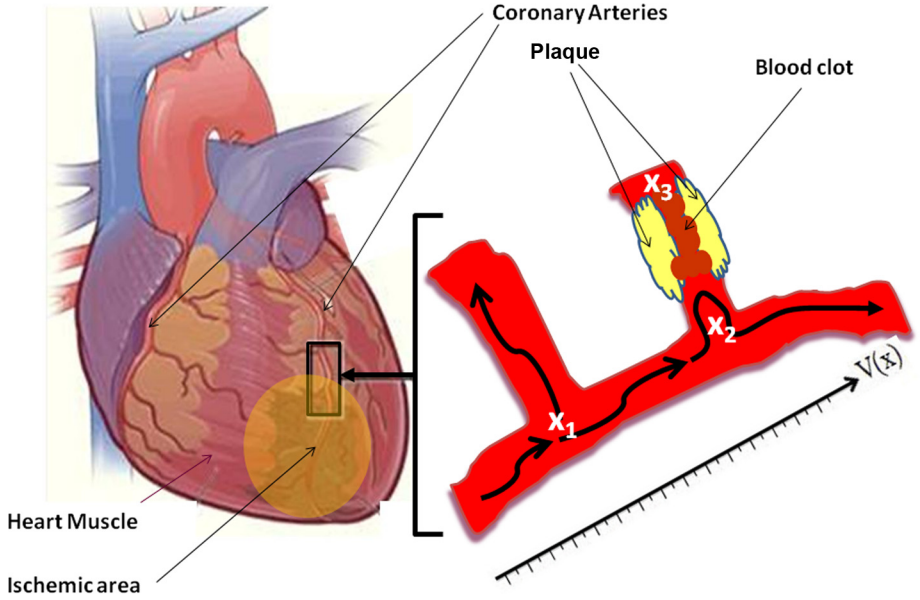

Figure 1. Illustration of the changes occurring in an ischemic cardiovascular accident and geometrical consideration in coronary artery with atherosclerosis diseases.

From equations (10), we can write:

$$\frac{d^2M_y}{dx^2} + \frac{1}{l}Cot\frac{x}{l}\frac{dM_y}{dx} + \frac{1}{l^2}n(n+1)M_y = 0 \quad (11)$$

$$Sin\frac{x}{l}\frac{d^2M_y}{dx^2} + \frac{1}{l}Cos\frac{x}{l}\frac{dM_y}{dx} + \frac{1}{l^2}Sin\frac{x}{l}n(n+1)M_y = 0 \quad (12)$$

$$\frac{d}{dx}\left(Sin\frac{x}{l}\frac{dM_y}{dx}\right) + \frac{1}{l^2}Sin\frac{x}{l}n(n+1)M_y = 0 \quad (13)$$

If we define $\varepsilon = Cos\frac{x}{l}$, equation (13) becomes

$$\frac{d}{d\varepsilon}\left\{(1-\varepsilon^2)\frac{dM_y}{d\varepsilon}\right\}\frac{1}{l^2}Sin\frac{x}{l} + \frac{1}{l^2}Sin\frac{x}{l}n(n+1)M_y = 0 \quad (14)$$

Dividing equation (14) through by $\frac{1}{l^2}Sin\frac{x}{l}$, we obtain a Legendre differential equation:

$$\left(1-\varepsilon^2\right)\frac{d^2M_y}{d\varepsilon^2} - 2\varepsilon\frac{dM_y}{d\varepsilon} + n(n+1)M_y = 0 \quad (15)$$

The solution of equation (15) is of the form:[13–16]

$$M_y(\varepsilon) = M_{yn}(\varepsilon) = C_1P_n(\varepsilon) + C_2Q_n(\varepsilon)\Big|_{n=0,1,2,3,\ldots} \quad (16)$$

where $P_n(\varepsilon)$ and $Q_n(\varepsilon)$ are the Legendre polynomials of the first type and second type, respectively, and C_1 and C_2 are constants. It is worthy of note that $P_n(\varepsilon)$ and $Q_n(\varepsilon)$ are two linearly independent solutions to equation.[15] Hence, C_2 must be equal to zero and C_1 is equal to unity:

$$M_{yn}(\varepsilon) = P_n(\varepsilon) = \sum_{p=0}^{\Theta}\frac{(-1)^p(2n-2p)!}{2^n\,p!(n-p)!(n-2p)!}\varepsilon^{n-2p} \quad (17)$$

where

$$\Theta = \frac{2n + \left((-1)^n - 1\right)}{4} \quad (18)$$

Equation (17) can be factorized by its own first term. Setting $m = n - p$:

$$M_{yn}(\varepsilon) = \frac{(2n)!}{2^n n!n!} \times\left\{\sum_{p=0}^{\xi(n)}(-1)^p\frac{(n-4p)}{p!}\frac{(n-p-1)!}{(n-2p)!}\varepsilon^{n-2p}\right\} = \frac{(2n)!}{2^n\,n!n!}B_n\left(\cos\frac{x}{l}\right) \quad (19)$$

where $B_n(\varepsilon)$ denote the Boubaker polynomials.[6–9]

$$\begin{aligned} B_0(\varepsilon) &= 1 \\ B_1(\varepsilon) &= \varepsilon \\ B_2(\varepsilon) &= \varepsilon^2 + 2 \\ B_3(\varepsilon) &= \varepsilon^3 + \varepsilon \\ B_4(\varepsilon) &= \varepsilon^4 - 2 \\ B_5(\varepsilon) &= \varepsilon^5 - \varepsilon^3 - 3\varepsilon \end{aligned} \quad \text{or} \quad \begin{aligned} B_0 &= 1 \\ B_1 &= \cos\frac{x}{l} \\ B_2 &= \left(\cos\frac{x}{l}\right)^2 + 2 \\ B_3 &= \left(\cos\frac{x}{l}\right)^3 + \left(\cos\frac{x}{l}\right) \\ B_4 &= \left(\cos\frac{x}{l}\right)^4 - 2 \\ B_5 &= \left(\cos\frac{x}{l}\right)^5 - \left(\cos\frac{x}{l}\right)^3 - 3\left(\cos\frac{x}{l}\right) \end{aligned} \quad (20)$$

$B_n(\varepsilon)$ is a polynomial in ε. The elementary first n-indexed solutions are represented in Figure 3.

Discussion

In Figure 3, the curves correspond to the vanishing modes of the expression obtained for the transverse magnetization in Equations (17) and (19). This feature agrees with the results obtained by Kobayashi et al,[16] Chapman et al,[17] and Donnat et al.[18]

The case $n = 0$ (Fig. 3) initially corresponds to the reduced equation:

$$\left(1-\varepsilon^2\right)\frac{d^2M_y}{d\varepsilon^2} - 2\varepsilon\frac{dM_y}{d\varepsilon} = 0 \quad (21)$$

which has the solution:

$$M_y(\varepsilon) = G_1 - \frac{G_2}{2}\ln\frac{1+\varepsilon}{1-\varepsilon} \quad (G_1 \text{ and } G_2 \text{ are constants}) \quad (22)$$

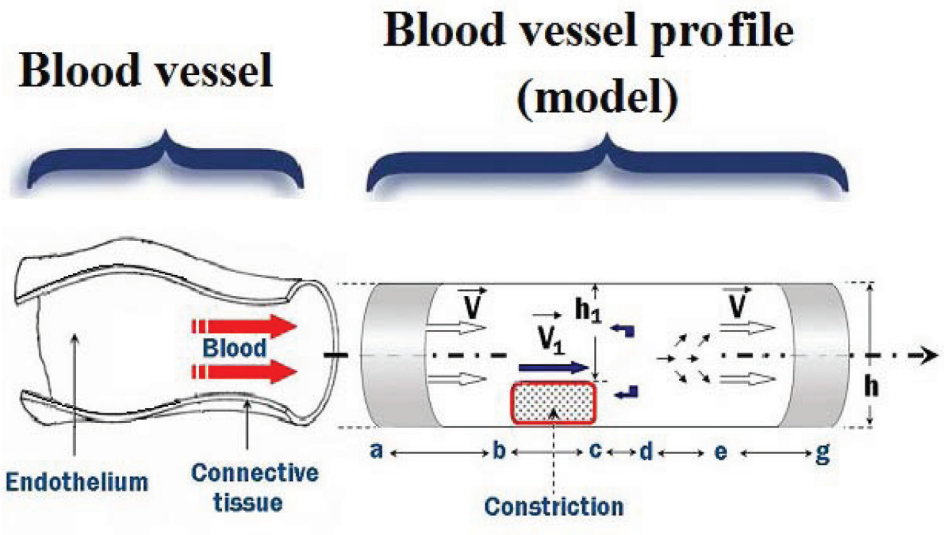

Figure 2. Effect of constriction on the velocity profile in a blood vessel: (ab) Laminar flow velocity *V*, (bc) High velocity V_1, (de) Turbulent, and (eg) Laminar flow. The diameter of the blood vessel is *h*.[21] Reprinted with permission of the Collegium Basilea.

It is interesting to note that whether the blood flow is laminar or turbulent, a magnetic resonance signal is always available. Specifically, at bifurcations and points just after the build-up of fatty deposits (sections d and e in Fig. 2) the transverse magnetization M_y is a constant. This indicates that resonant waves can be reconstructed to image the points within the blood vessels where flow is turbulent. Figures 3 and 4 suggest that except at points where there is no contribution from velocity, transverse magnetization must be continuous. That is, M_y cannot jump from one value to another. We therefore set the boundary condition for the fluid particle:

$$M_y = G_1 \text{ at } x = \frac{\mu\pi l}{2} \ (\mu = 1,3,5,7,9.....) \qquad (23)$$

Equation (7) shows that an acceptable solution of equation (6) according to the assumptions made above can only be obtained if the fluid particle has certain discrete values μ, an NMR number associated with the NMR transverse magnetization and velocities. It is very important to note that this parameter is very related to the nature of flow observed within the vessels.

Figures 3 and 4, show the effect of the values of *n* on both Boubaker polynomial B_n and the NMR transverse magnetization M_y. They show the behavior of the NMR signal at several points within the vessel being observed. Notably, Figure 4 demonstrates the importance of the ratio $\frac{x}{l}$. When the value of this term (corresponding to a small distance along the blood vessel as weighted against *l*) is very small (Fig. 4f), there is no significant NMR contrast between different points within an in homogeneous voxel. Hence, to observe a significant signal at any location, *l* must be tuned to the corresponding ranges of values; these values can therefore be introduced into k–space encoding the spatial information. We also see that

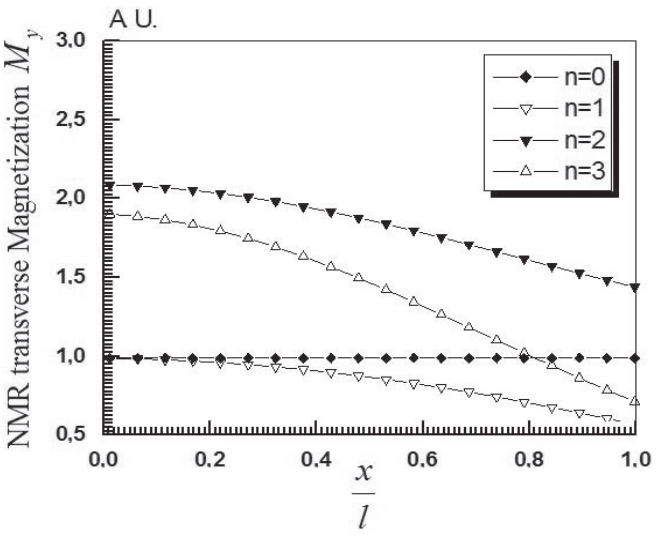

Figure 3. The n-indexed solutions.

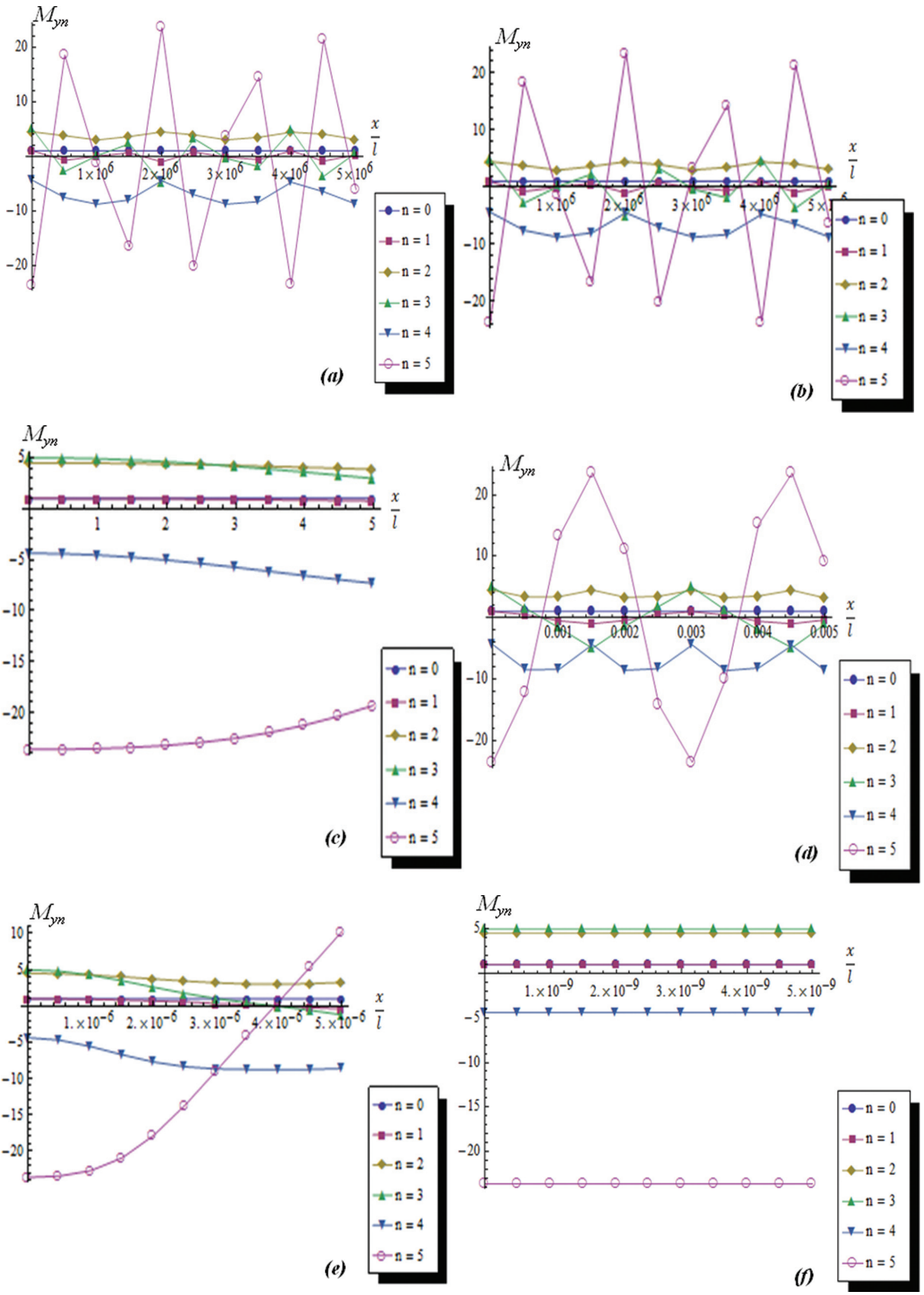

Figure 4. Plots of transverse magnetization as a function of $\frac{x}{l}$ at l = 2.5 μm for x between 0 and (**a**) 1.0 m (**b**) 1.0×10^{-3} m (**c**) 1.0×10^{-6} m (**d**) 1.0×10^{-9} m (**e**) 1.0×10^{-12} m (**f**) 1.0×10^{-12} m.

this formulation allows us to sample NMR signals at extremely small values of x, which may be important for better characterization of plague size and morphology.

Studying the Legendre and Boubaker solutions to the Bloch NMR flow equation for the behavior of NMR signals in flowing media is invaluable because it can allow effective monitoring of geometrical and morphological situations in the arteries as well as the possible effect of drugs on cardiovascular related diseases in any tissue. Based on earlier studies,[22–24] $l(x)$ may be defined in the Cartesian cylindrical and spherical coordinates as shown in Figure 2, where $l(x) = h - h_1$. When $n = 0$ and the vessel is not completely blocked, the flow is extremely complex. Values for $n > 0$ indicate that the size of h_1 is drastically reducing and the velocity $V(x)$ is becoming more laminar (steady) in oxygenated blood and cerebrospinal fluid (CSF) as shown in Figure 5. The value of n can be used to indicate the efficacy of any drug useful for reducing plaque size, as shown in Figure 5.

Similarly, equation (10) can be significantly valuable for estimating blood flow of blood vessels with very small cross section area $A = l^2(x)$, where the value of n may be defined as $0 < n < 5$.

Figure 6 shows the distribution plots for the fluid velocity and the corresponding density plots for different ranges of l. These figures show that the study affords us the opportunity of simultaneously adding velocity mapping to MRI of blood flow within the vessels. The points with white open areas are points at which complex or turbulent flow occurs. These points typically coincide with presence of bifurcations and fatty deposits. Additionally, as l becomes microscopic and lower, the model becomes more realistic. The points with sharp peaks or the red regions on the density image correspond to highest values of fluid velocity and can be used to determine and also image the presence of fatty deposits.

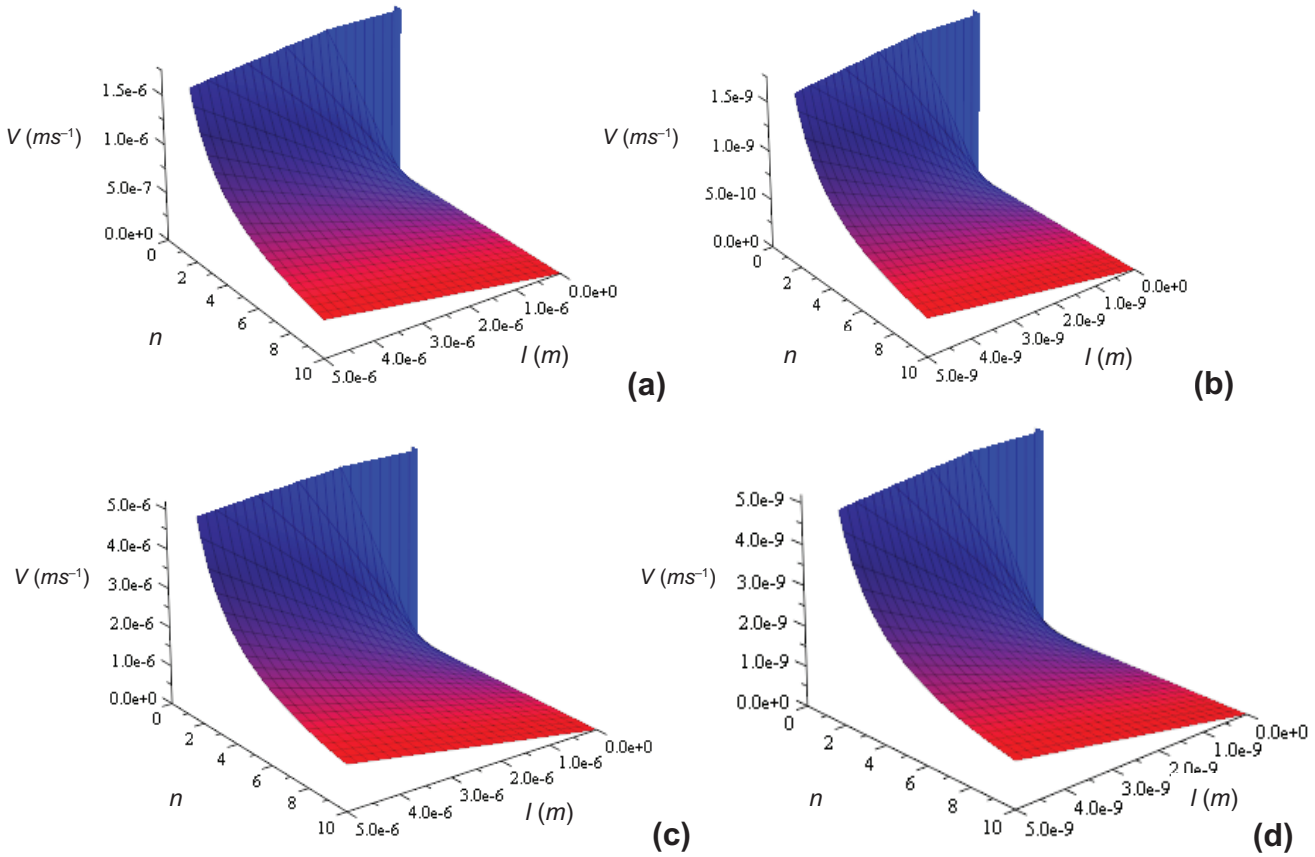

Figure 5. The plots of the fluid velocity for molecules of (**a**) cerebrospinal fluid around a "micro-sized" plague (**b**) cerebrospinal fluid around a "nano-sized" plague (**c**) oxygenated blood around a "micro-sized" plague (**d**) oxygenated blood around a "nano-sized" plague.

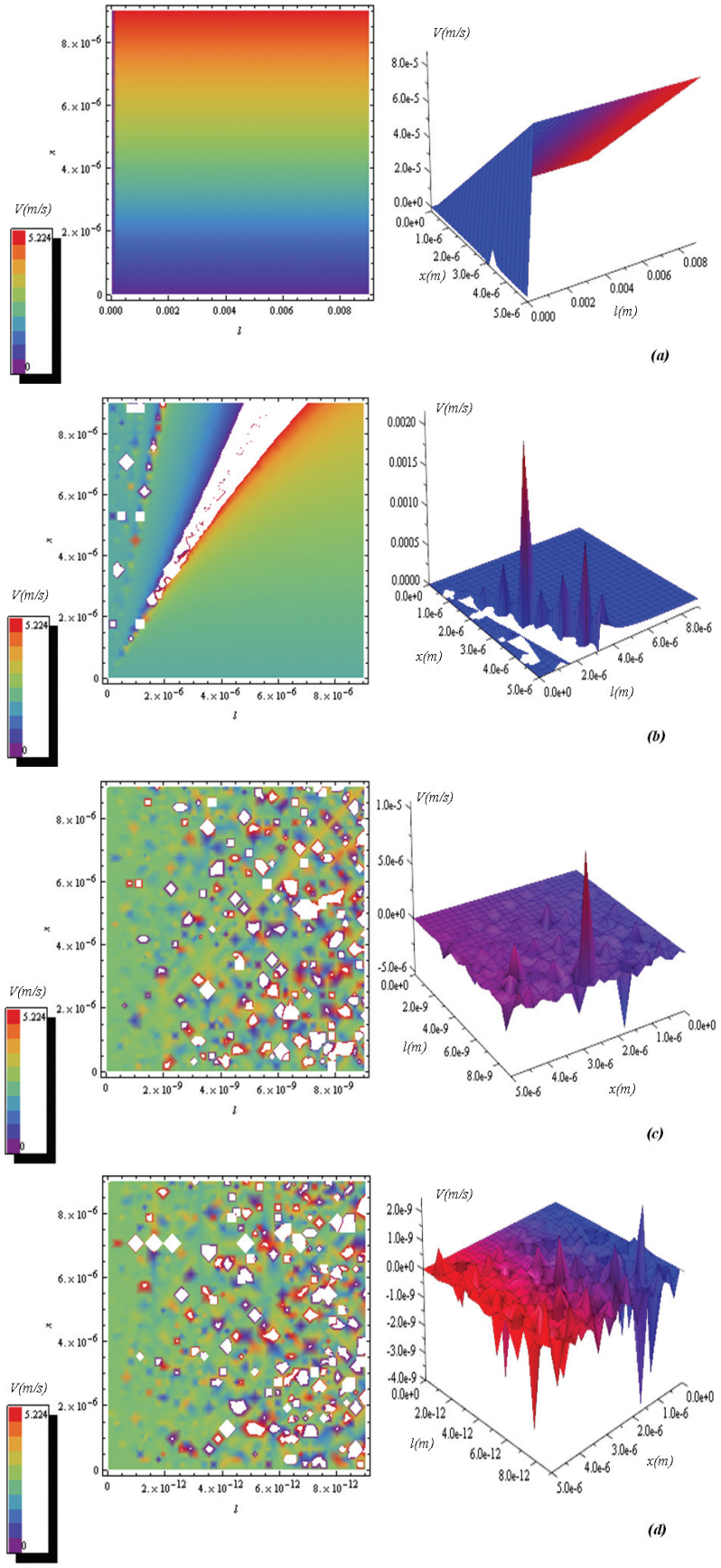

Figure 6. The velocity distribution across *l* and *x*, according to equation (7) and the corresponding density image for *l* ranging from 0 to (**a**) 9.0×10^{-3} m (**b**) 9.0×10^{-6} m (**c**) 9.0×10^{-9} m (**d**) 9.0×10^{-12} m. The relaxations times used are $T_1 = 1.03$s and $T_2 = 0.06$s.

It may be significant to note that the rotational diffusion coefficient D_{rot} can be defined from equation (7) as,[19,20] considering that l is a fixed length:

$$D_{rot} = \frac{V^2(x)}{l^2 T_g \tau} \tag{24}$$

Given that the translational diffusion coefficient is: $D_{trans} = \frac{V^2(x)}{T_g \tau}$, where τ is the correlation time defined as:[19,20]

$$\tau = \frac{1}{n(n+1) D_{rot}} \tag{25}$$

For the value $n = 1$, $M_y(\varepsilon) = P_1(\varepsilon) = B_1(\varepsilon)$ and the correlation time becomes

$$\tau = \frac{1}{2D_{rot}} \tag{26}$$

The physical implication for when $n = 0$ can be interpreted as the constant magnetization where the correlation time is observed to be infinitely small.

Finally, the rotational diffusion coefficient as given in equation (23) may be written as:[19,20]

$$\frac{V^2(x)}{l^2 T_g \tau} = \frac{k_B T}{f_r}$$

where k_B is the Boltzman n constant, T is the absolute temperature of the tumbling blood molecules, and f_r is the rotational friction coefficient. Therefore, the friction coefficient, which provides significant information regarding molecular interactions, is given as:

$$f_r = k_B T T_g \tau [n(n+1)] = \frac{k_B T T_g \tau}{T_0^2} \cot^2 \frac{x}{l} \tag{27}$$

Conclusions

We have derived the MRI signal in terms of Legendre and Boubaker polynomials. By solving the Bloch NMR flow equations under some assumptions, we obtained elementary spatial profiles of the transverse magnetization response. The primary advantage of this approach is the potential to exploit spatial-evolution of magnetic response in the presence of a preset rotating field for monitoring the effect of a drug on cardiovascular-related diseases and to estimate blood flow rate in very small blood vessels.

Interestingly, quantification of the velocity is not a direct prediction of equation (7), but it is a consequence of the conditions imposed on the transverse magnetization.

In physical situations in which a fluid particle is confined in space, for example, at $x = \beta l$, $\left(\text{where } -\frac{\pi}{2} < \beta < +\frac{\pi}{2}\right)$, most solutions behave in an inappropriate way at the edges of the region of interest. Only for certain precisely determined velocities are satisfactory solutions obtained. The boundary conditions which the transverse magnetization M_y must satisfy cannot be derived. They can be justified in part by the physical interpretation of M_y based on the properties of Boubaker polynomials in equation (19):

(i) M_y must be a well-defined functions of position,
(ii) M_y cannot be infinite any where except at the point $x = \frac{\mu\pi l}{2}$ (μ = even integer),
(iii) M_y must be continuous, and not jump abruptly from one value to another.
(iv) When $n = 0$, and $x = \frac{\mu\pi l}{2}$ (μ = odd integer), the transverse magnetization is a constant and the velocity is indeterminate.
(v) The NMR transverse magnetization is directly proportional to Boubaker polynomials.
(vi) M_y has the same value as the Boubaker polynomials when $n = 1$.

Detailed study of these NMR flow parameters and properties of the transverse magnetization as described in this study can allow for careful optimization and 3D computer graphics of fluid flow magnetic resonance imaging. A simple illustration of this is given in Figure 6. The mathematical analysis presented in this study is based on the assumption made in equation (7). This was done with the goal of exploring the spatial evolution of the MRI signal in the presence of a preset rotating field.

The biological, physical, biomedical, and geophysical applications of equations (17), (19), (23), (25), and (27) when $n > 1$ can be used for all NMR/MRI procedures and further application of this study will be presented in separate studies. For an example of the physical properties of a drug designed to reduce the size of h_1 of the fatty deposit in Figure 2 may be revealed by equations (24–27).

Notably, the parameter l in equation (7) is a length used to scale x. This parameter may be used for slice selection in spatial encoding in a typical MRI experiment so that l can be defined such that:

$$l = \frac{1}{\gamma G \tau} \tag{28}$$

where G is the applied gradient and τ is the duration of the applied gradient.[4] The area $A = l^2\,(x)$ (which was discussed above) represents the field of view (FOV) for the voxel selected.

Author Contributions

DOM, AOB, AOA and BK participated equally in the work giving rise to this manuscript. All authors reviewed and approved of the final manuscript.

Acknowledgement

The authors acknowledge the support of Federal University of Technology Minna through the STEP—B research scheme. The meticulous review of this article is highly appreciated.

Competing Interests

Authors disclose no potential conflicts of interest.

Disclosures and Ethics

As a requirement of publication the authors have provided signed confirmation of their compliance with ethical and legal obligations including but not limited to compliance with ICMJE authorship and competing interests guidelines, that the article is neither under consideration for publication nor published elsewhere, of their compliance with legal and ethical guidelines concerning human and animal research participants (if applicable), and that permission has been obtained for reproduction of any copyrighted material. This article was subject to blind, independent, expert peer review. The reviewers reported no competing interests.

References

1. Ngo JT, Morris PG. General solution to the NMR excitation problem for non-interacting spins. *Magn Reson Med*. 1987;5(3):217–237.
2. Rourke DE, Morris PG. The inverse scattering transform and its use in the exact inversion of the Bloch equation for non-interacting spins. *Journal of Magnetic Resonance*. 1992;99(1):118–138.
3. Rourke DE, Morris PG. Half solitons as solutions to the Zakharov-Shabat eigenvalue problem for rational reflection coefficient with application in the design of selective pulses in nuclear magnetic resonance. *Phys Rev A*. 1992;46(7):3631–3636.
4. Cowan BP. (1997). Nuclear Magnetic Resonance and Relaxation, 1sted. Cambridge: Cambridge University Press.
5. Awojoyogbe OB, Dada OM, Faromika OP, Dada OE. Mathematical concept of the Bloch flow equations for general magnetic resonance imaging: are view. *Concepts in Magnetic Resonance Part A*. 2011;38A(3):85–101.
6. Dada OM, Faromika OP, Awojoyogbe OB, Dada OE, Aweda MA. The impact of geometry factors on NMR diffusion measurements by the Stejskal and Tanner pulsed gradients method. *International Journal of Theoretical Physics, Group Theory and Nonlinear Optics*. 2011;15(1–2).
7. Awojoyogbe OB. Analytical solution of the time-dependent Bloch NMR equations: atranslational mechanical approach. *Physica A*. 2004;339(3–4): 437–460.
8. Awojoyogbe OB, Boubaker K. A solution to Bloch NMR flow equations for the analysis of homodynamic functions of blood flow system using m-Boubaker polynomials. *Current Applied Physics*. 2009;9(1):278–283.
9. Boubaker K. On modified Boubaker polynomials: some differential and analytical properties of the new polynomials issued from an attempt for solving bi-varied heat equation. *Trends in Applied Science Research.* 2007;2(6):540–544.
10. Labiadh H, Boubaker K. A Sturm-Liouville shaped characteristic differential equation as a guide to establish a quasi-polynomial expression to the Boubaker polynomials. *Journal of Differential Equations and CP*. 2007;2:117–133.
11. Labiadh H, Dada M, Awojoyogbe OB, Ben Mahmoud KB, Bannour A. Establishment of an ordinary generating function and a Christoffel-Darboux type first-order differential equation for the heat equation related Boubaker-Turki polynomials, *Journal of Differential Equations and CP*. 2008;1:51–66.
12. Antonov VA, Timoshkova EI, Kholoshevnikov KV. *An Introduction to Theory of Newton's Potential* [in Russian]. Moscow: Nauka, 1988.
13. Suetin PK. *Classical Orthogonal Polynomials* [in Russian]. 2nd ed. Moscow: Nauka, 1979.
14. Gradshteyn IS, Ryzhik IM. *Tables of Integrals*, *Series*, *and Products* [in Russian]. 2nd ed. Waltham, MA: Academic Press, 1994.
15. Bateman H, Erd´elyi A. *Higher Transcendental Functions*, vol. 3: *Elliptic and Modular Functions*. *Lame and Mathieu Functions*, New York, NY: McGraw–Hill, 1955; Russian transl: Moscow, 1967.
16. Kobayashi A, Okayama Y, Yamazaki N. ^{31}P-NMR magnetization transfer study of reperfused rat heart. *Mol Cell Biochem*. 1993;119(1–2):121–127.
17. Chapman BE, Kuchel PW. Fluoride trans membrane exchange in human erythrocytes measured with ^{19}F NMR magnetization transfer. *Eur Biophys J*. 1990;19(1):41–45.
18. Donnat P, Rauch J. Global solvability of the Maxwell-Bloch equations from nonlinear optics. *Archive for Rational Mechanics and Analysis*. 1996; 136:291–303.
19. Loman A, Gregor I, Stutz C, Mund M, Enderlein J. Measuring rotational diffusion of macromolecules by fluorescence correlation spectroscopy. *Photochem Photobiol Sci.* 2010;9(5):627–636.

20. Martínez MC, García de la Torre J. Brownian dynamics simulation of restricted rotational diffusion. *Biophys J*. 1987;52(2):303–310.
21. Dada M, Awojoyogbe OB, Moses FO, Ojambati OS, De DK, Boubaker K. A mathematical analysis of stenosis geometry, NMR magnetizations and signals based on the Bloch NMR flow equations, Bessel and Boubaker polynomial expansions. *Journal of Biological Physics and Chemistry*. 2009;9(3):101–106.
22. Awojoyogbe OB. A mathematical model of Bloch NMRequations for quantitative analysis of blood flow in blood vessels with changing cross-section II. *Physica A*. 2003;323(C):534–550.
23. Awojoyogbe OB. A mathematical model of Bloch NMR equations for quantitative analysis of blood flow in blood vessels with changing cross-section I. *Physica A*. 2002;303:163–175.